UDC 621.777 DOI: 10.37142/2076-2151/2025-1(54)21

Titarenko A.
Hornostai V.
Sviatskyi Y.
Lipodat V.

THE EFFECT OF STAMPING TEMPERATURE IN STAMPING FULL HIGH-CARBON STEEL PRODUCTS

In the engineering production of hollow products, hot and incomplete hot deformation is used. The main technologies used to manufacture hollow products are forging, stamping and specialized metal forming processes (MFP). The main advantages of the MFP processes compared to casting processes are: minimal material consumption, high quality of the material and workpiece surfaces (stamping and rolling processes on rolling mills), shape and dimensional accuracy, high productivity, and the ability to mechanize and automate production processes. MFP at the current stage of development of machine manufacturing technology is one of the main methods for producing parts.

In particular, when manufacturing hollow products in modern conditions, there is an urgent need to determine the parameters of the stamping tooling, its characteristics, technological transitions, temperature conditions for processing semi-finished products and their mutual influence on the finished product. These issues have been considered and continue to be considered by various authors, so the research topic is relevant. In the proposed work, a finite element modeling of the process of extrusion of hollow products from high-carbon steel (AISI-1060) under hot and incomplete hot deformation was performed. A comparison of the processes of reverse extrusion under hot and incomplete hot deformation was also performed with the appropriate formulation of the problem for modeling the process of reverse extrusion under hot and incomplete hot deformation. The analysis of the results of the extrusion simulation allows us to determine the characteristics of the resulting product and reduce the time for process development. The heating temperature of the workpiece for modeling extrusion under hot deformation was 1000 °C, and for modeling extrusion under incomplete hot deformation, the temperature was 700 °C. These temperatures were determined using a state diagram, at a temperature above 760 °C, complete recrystallization of the metal occurs, which is characteristic of hot deformation processes, at a deformation temperature below 760 °C, incomplete recrystallization crystallization occurs, which characterizes an incomplete hot deformation process. The modeling results are the dependence of the extrusion force on the punch displacement, the values of normal stresses, which are used to determine the specific forces on the contacting surfaces between the workpiece and the deforming tool, to determine the temperature distribution at the end of the process of reverse extrusion, and to consider the distribution of the stress and strain state. The press equipment, final shape and dimensions of the semi-finished product are determined.

Keywords: *finite element method, hot deformation, incomplete hot deformation, extrusion during hot deformation, extrusion during incomplete hot deformation, hollow semi-finished products, forces, specific forces, stresses, deformations, temperature distribution, extrusion scheme.*

In the production of hollow products of various shapes and sizes, extrusion processes are often used during hot and incomplete hot deformation. These processes are considered by the authors [1–2], which describe recommendations for deformation and design of die tooling. When deforming hollow products, the processes of incomplete hot and hot deformation must take into account the resulting energy-force parameters and specific forces. These processes are described in the following sources [3–4]. A critical analysis of the serial technology for producing forgings of the aircraft hydraulic cylinder cover type was carried out and, using the developed technique, the possibility of internal cracking was established. A technology for stamping a cover made of Amg6 alloy in a closed die cavity is proposed, which provides not only a significant increase. An assessment of the required stamping force by transitions was carried out. The validity of the proposed technology was confirmed by physical experiments. An analysis of the macrostructure was carried out using a scanning electron microscope and measurements of the Brinell rigidity of forgings obtained by multi-transition stamping. Based on the conducted research, technological recommendations for hot multi-pass closed stamping of critical aircraft parts were formulated [5].

The aim of the study by the authors [6] is to study the influence of tool geometry on the wear characteristics of the mandrel and matrix surfaces. The paper examines the influence of two main process parameters on the wear of SCM415H steel: the height of the annular gap and the diameter of the mandrel.

When studying the deformation process, computer modeling is used using the finite element method (FEM) and the DEFORM software package. Thanks to modeling, it is possible to determine the technological parameters of the process, such as temperature distribution, energy-force parameters, specific forces, stress and strain state, and the final shapes and dimensions of the product, information on which is presented in sources [7–8].

The authors [9] investigated a combined extrusion process that simultaneously combines the main extrusion processes such as direct and reverse extrusion (squeezing). In this paper, the production of a relay housing for the automotive industry was analyzed. In order to reduce the force, plastic deformation work, the number of process stages and to increase the ductility of low-carbon steel C15, the so-called semi-hot extrusion process was used. The study was carried out using a pilot production tool with a strain gauge and finite element modeling.

Reducing the forming force and removing the ejector pin, improving the formability of sheet metal parts and producing high-strength parts are the main reasons for applying the hot stamping process, which were investigated by the authors in [10]. According to this study, the hot stamping process of 22MnB5 steel is a state-of-the-art process, but new processes and steel grades are also considered in the work. The current study characterized the behavior of MSW1200 steel blanks in the semi-hot and fully hot stamping processes. In the semi-hot stamping process, the blank was first heated to a temperature of about 650 °C, then simultaneously formed and quenched in the die. The microstructure and mechanical properties of the semi-hot stamped and fully hot stamped blanks were studied and the results were compared with those of the water/air quenched blanks. The hot stamped blanks achieved the same strength values as the water quenched blanks. The highest plasticity and, accordingly, the best forming were achieved in the semi-hot stamped blank. It was concluded that for the steel under consideration, the semi-hot stamping process can be considered as an improved thermomechanical process, which not only guarantees high formability, but also leads to obtaining ultra-high strength properties.

The authors [11] argue that the mechanical properties of extruded AlMgSi alloys depend on the applied thermomechanical parameters used throughout the manufacturing process. Below, the effects of different extrusion speeds and homogenization conditions in combination with air or water quenching are investigated on four different sets of AA6082-T4 rectangular hollow sections. These sections were manufactured and extruded under industrial conditions, and selected cross-sections of each section were examined using optical microscopy to determine the microstructure and level of recrystallization. In addition, samples with recrystallized microstructure generally exhibited a higher standard deviation of mechanical properties, which may lead to product quality and consistency issues for metal forming operations. The authors provide a deeper understanding of how the selected thermomechanical parameters affect the final properties of such sections. Aluminium alloys such as AlMgSi are commonly used for extruded profiles as this allows control of cross-sectional geometry while using material efficiently.

In the article [12] the authors present a universal kinematic module developed on the basis of the upper boundary method, intended for use in mathematical modeling of combined cold extrusion processes. In particular, this module can be used to model the force mode and analyze tool loads during radial-direct extrusion of hollow products with a blind hole from solid blanks to describe deformation zones during metal flow to the center and to rotation zones from the radial flow back. Analytical dependencies are obtained for the power of the deformation forces, friction and displacement at the module boundaries, as well as for the reduced pressure in parametric form.

In [13], a generalized analytical approach based on the slab analysis method is developed for analyzing the mechanics of extrusion of an axisymmetric pipe from a hollow or solid round blank for a fairly general case of extrusion of a pipe through a profile head or through a profile mandrel. The results obtained as a result of theoretical analysis for the average extrusion force for various die-mandrel combinations are compared with experimental studies conducted on a model material and with the works of other authors [14, 15]. They show fairly good results.

The authors analyzed the mechanics of pressing an axisymmetric pipe, starting with a hollow or solid round blank. The authors developed a generalized analytical method based on the slab analysis method for a somewhat general case of pressing a pipe with a punch through a conventional profile matrix. As a result of the study, the authors determined the average pressing pressure, which was determined using theoretical analysis for various matrix-mandrel combinations. The article [15] also describes the results that are determined by experimental studies conducted on a model material.

The authors [16-20] demonstrated the possibilities of optimizing the design of hot extrusion dies, allowing for an accurate assessment of die wear during MCE. The presented articles present the results of the influence of thermal action on the rigidity of the tool material. The results of fundamental studies of changes in hardness due to thermoplasticity of the tool material are presented. To obtain the necessary data for calibrating the model, optical measurements were carried out on several industrial dies using statistical analysis. It is proven that the proposed model can be used to assess the wear of hot extrusion dies during cyclic stamping.

Study of the effect of deformation rate on the process of hot deformation of hollow products, described in the article [21]. The authors compare the results of deformation at different speeds of the punch using the MCE. The results of the study can be used to determine the optimal speed of the deforming tool for the process of deformation of hollow products.

An alternative method for producing hollow products is rotational deformation, described in the article [22]. The method consists of local deformation of the workpiece, which reduces the number of transitions in the manufacture of hollow products. However, rotational deformation has some disadvantages in production and the complexity of the tooling for deformation.

The aim – of the study is to substantiate the efficiency of reverse extrusion processes depending on the temperature of the workpiece. To consider the effect of the temperature of the workpieces on the process of extrusion of hollow products from high-carbon steel during hot and incomplete hot deformation.

Problem statement. Numerical experiments were conducted using finite element modeling of the extrusion process using the DEFORM software package. Fig. 1 shows the cross-sectional diagram of the part to be obtained (Fig. 1a), and Fig. 1b shows the original workpiece made of high-carbon steel AISI-1060.

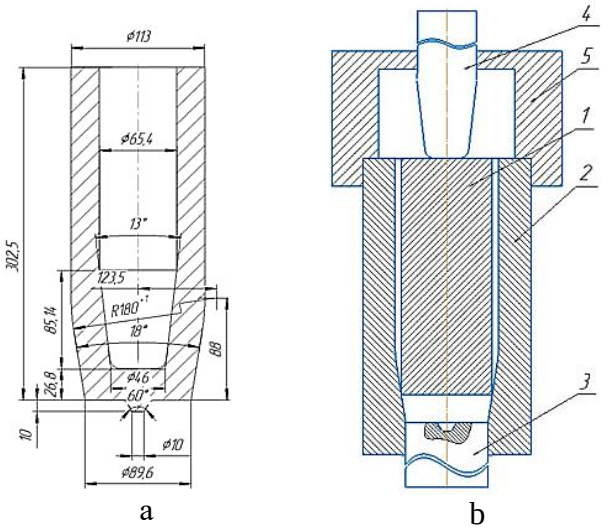

Fig. 1. Longitudinal section of the part (a), extrusion diagram (b) – centering ring 5, punch 4, matrix 2, ejector 3, workpiece 1.

The following parameters were used to simulate the deformation process:

- the temperature of the deforming tool is 20°C;
- The temperatures are set in accordance with the state diagram of steel C60. According to the diagram, at a temperature above 760 ℃, complete recrystallization of the metal occurs, which is typical of hot deformation processes. In the case of an incomplete hot deformation process, according to the crystallization diagram, the temperature should not exceed 760 ℃; The temperature of the original workpiece during the hot extrusion process is 1000 ℃, and under conditions of incomplete hot extrusion, the temperature is 700 ℃ [21];
- use centering ring 5 (Fig. 1b) for numerous experiments;
- for the process to proceed in the required temperature range, the speed of movement of the punch during deformation V_o = 100 mm/s [21];
- the coefficient of friction μ between the deforming tool and the workpiece is 0.25.

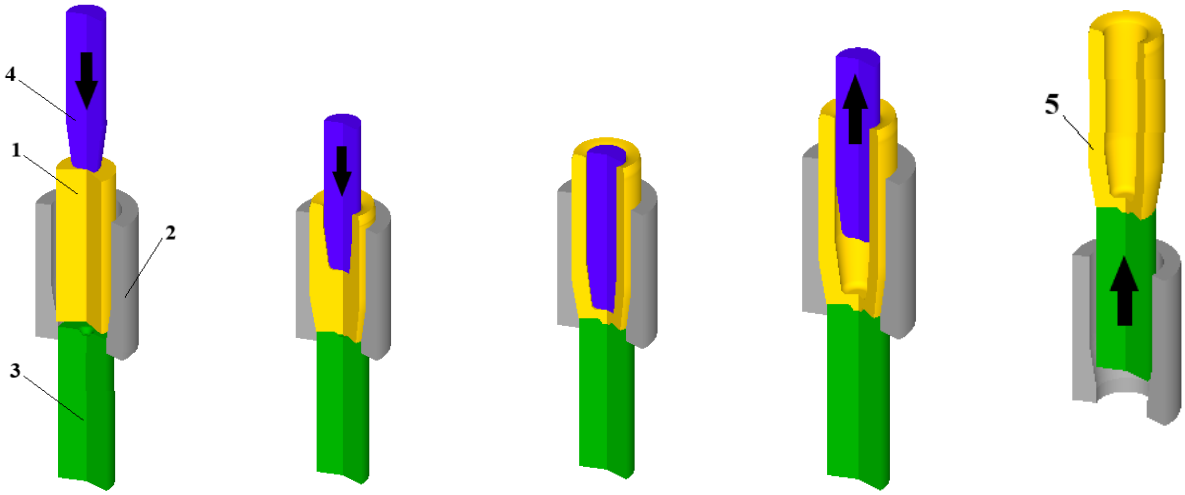

Fig. 2. Calculated positions in the cross-section of the deforming tool during reverse extrusion with upsetting (1 - workpiece, 2 - matrix, 3 - ejector, 4 - punch): a - at the beginning of extrusion, b - at an intermediate stage of extrusion, c - at the end of extrusion, d - after removal of the punch, e - after ejection of the product).

The extrusion process diagram is shown in Fig. 1b. The position of the tool during the deformation process at different stages of reverse extrusion with upsetting is shown in Fig. 2. At the first stage, Fig. 2a, we can observe the beginning of the extrusion process. The figure shows the workpiece 1 installed in the matrix 2 and on the ejector 3. Under the action of the slider, the punch 4 moves and deforms the workpiece 1. At the beginning of the deformation process, shown in Fig. 2b, the initial flow of the metal can be observed.

The end of the deformation process is shown in Fig. 2c. At this stage, the punch forms the final shape of the semi-finished product. One of the most important stages of the deformation process is the extraction of the working tools from the product and the extraction of the product from the tool. These stages are shown in Fig. 2d and Fig. 2e. After the deformation process shown in Fig. 2c, the punch 4 begins to move in the direction opposite to its movement during deformation, which is shown in Fig. 2d. The final stage of the process is the extraction of the semi-finished product 5 from the matrix 2 using the ejector 3, which is shown in Fig. 2e.

Results of the study. Analysis of the obtained results of modeling two deformation processes, namely: the dependence of the extrusion force on the displacement of the punch, the distribution of normal stresses, the distribution of temperature, the distribution of stress components in the deformed workpiece at the end of the reverse extrusion, the distribution of final axial ε_z, radial ε_r, tangential ε_θ, deformations and deformation intensity ε_i after extrusion.

The parameters of the force modes (Fig. 3) for reverse extrusion with upsetting under hot and incomplete hot extrusion conditions allow selecting the required pressing equipment. Under hot extrusion conditions, the force graph (Fig. 3a) has two sections: unsteady and steady. At the unsteady stage, the force increases and is 2200 kN when the punch moves by 170 mm. At the steady stage, the force increases and reaches a maximum value of 2410 kN when the punch moves by 259 mm. Next, we will consider the graph of the extrusion force versus the punch movement under incomplete hot extrusion conditions, shown in Fig. 3b. The graph of the extrusion force versus the punch movement under incomplete hot extrusion conditions has two sections: unsteady and steady, like the graph for hot deformation. At the unsteady stage, the deformation force increases to 3220 kN when the punch moves by 170 mm. At the next stage, the force increases and reaches a maximum value of 3378 kN at the end of the extrusion process when the punch moves by 259 mm.

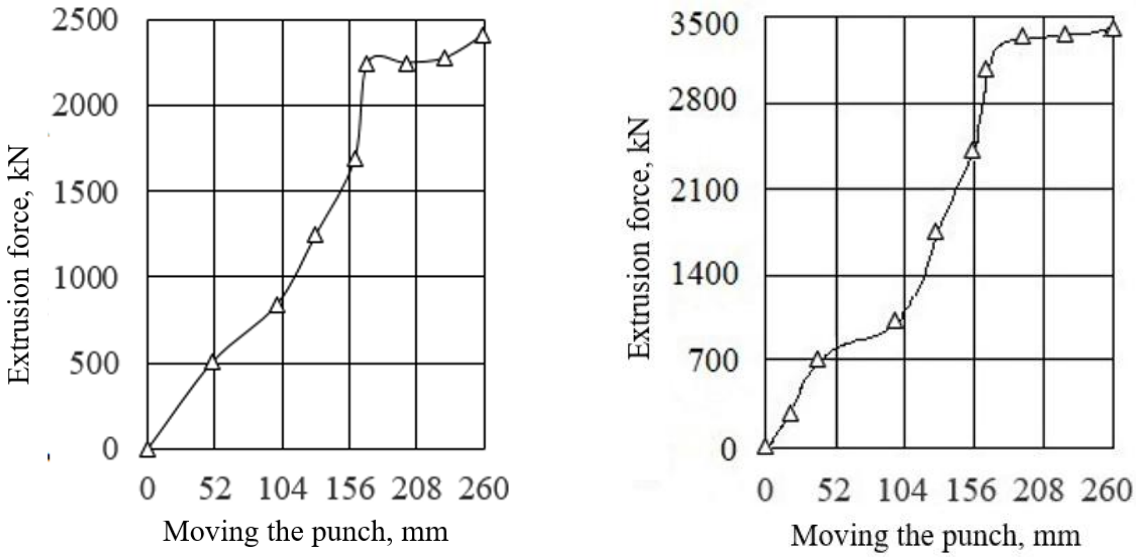

a b

Fig. 3. Dependence of the extrusion force on the displacement of the punch:
a – under hot extrusion conditions; b – under incomplete hot extrusion conditions

The distribution of normal stresses σ_n, that characterize the distribution of specific forces between the contact surface of the workpiece and the deforming tool, is shown in Fig. 4. The obtained data are necessary when designing stamping equipment.

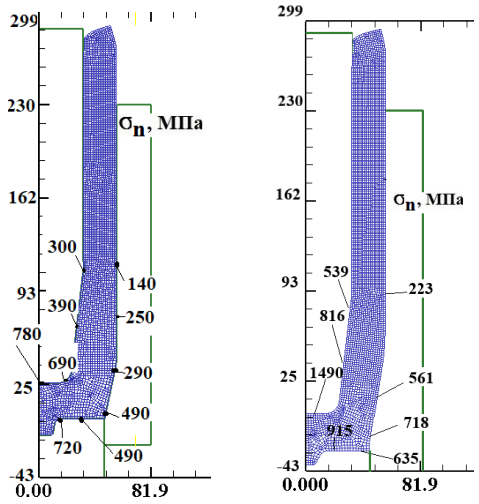

a b

Fig. 4. Distribution of normal stresses: a – under hot extrusion conditions, b – under incomplete hot extrusion conditions.

The distribution of normal stresses under hot extrusion conditions was analyzed first and is shown in Fig. 4a. As can be seen from the distribution of normal stresses at the contact point of the punch and the workpiece, the normal stress is within the range of $\sigma_n = 300 \div 780$ MPa. In the contact zone of the die and the workpiece, the normal stresses are within the range of $\sigma_n = 140 \div 490$ MPa, and at the contact point of the ejector and the workpiece $\sigma_n = 490 \div 720$ MPa. For incomplete hot extrusion, the distribution of normal stresses is shown in Fig. 4b. At the contact point of the punch and the workpiece, the normal stress is within the range of $\sigma_n = 539 \div 1490$ MPa. In the contact zone of the die and the workpiece, the normal stresses are within the range of $\sigma_n = 23 \div 718$ MPa, and at the contact point of the ejector and the workpiece $\sigma_n = 635 \div 915$ MPa.

The temperature distribution in the volume of the deformed product material at the end of the reverse extrusion process with upsetting under hot and incomplete hot deformation conditions is shown in Fig. 5. Thanks to this distribution, it is possible to analyze the temperature after deformation for further planning of operations.

Under hot extrusion conditions, the temperature distribution shown in Fig. 5a. It is evident from the distribution that the temperature in the wall reaches T = 940 ÷ 1000 ºC. In the metal layers on the side of the internal cavity of the workpiece, the temperature is T = 940 ºC, and in the metal layers on the side of the external surface of the workpiece, the temperature is T = 740 ºC. Under incomplete hot extrusion conditions, the temperature distribution shown in Fig. 5b was obtained. It is evident from the distribution that the temperature in the wall reaches T = 697 ÷ 700 ºC. In the metal layers on the side of the internal cavity of the workpiece, the temperature is within the range of

T = 490 ÷ 649 ºC, and in the metal layers on the side of the external surface of the workpiece, the temperature is within the range of T = 280 ÷ 500 ºC.

The stress-strain state of the material at the end of the process of reverse extrusion with upsetting under hot and incomplete hot deformation conditions is considered, which is shown in Fig. 6 and Fig. 7. The distributions of axial stresses σ_z, radial stresses σ_r, tangential stresses σ_θ and stress intensity σ_i for the process of hot reverse extrusion are shown in Fig. 6. At the punch end, in the places of the conical parts of the matrix and punch, the axial stresses σ_z (Fig. 6a), tangential stresses σ_θ (Fig. 6c) and radial stresses σ_r (Fig. 6b) have a compressive nature of stresses, which significantly decreases in the cylinder. In the bottom part of the punch, the axial stresses shown in Fig. 6a are within σ_z = - 360 ÷ -840 MPa. The radial stresses shown in Fig. 6b are within the range σ_r = - 380 ÷ - 730 MPa. The tangential stresses shown in Fig. 6c are within the range σ_θ = - 370 ÷ - 660 MPa.

In this case, the distribution pattern of radial stresses σ_r and tangential stresses σ_θ is almost the same. The deformation center during extrusion with thinning is located in the bottom part of the deformed workpiece,

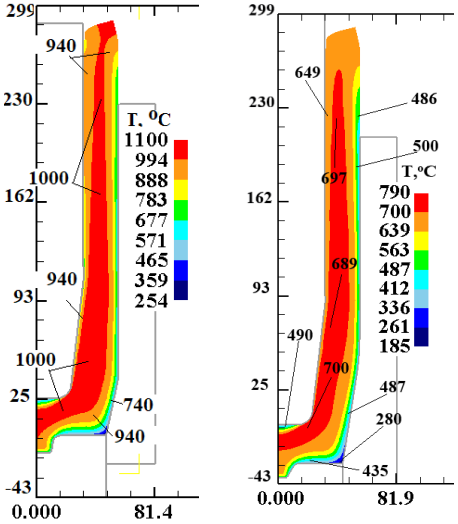

a b

Fig. 5. Temperature distribution:
a – under hot extrusion conditions,
b – under incomplete hot extrusion conditions.

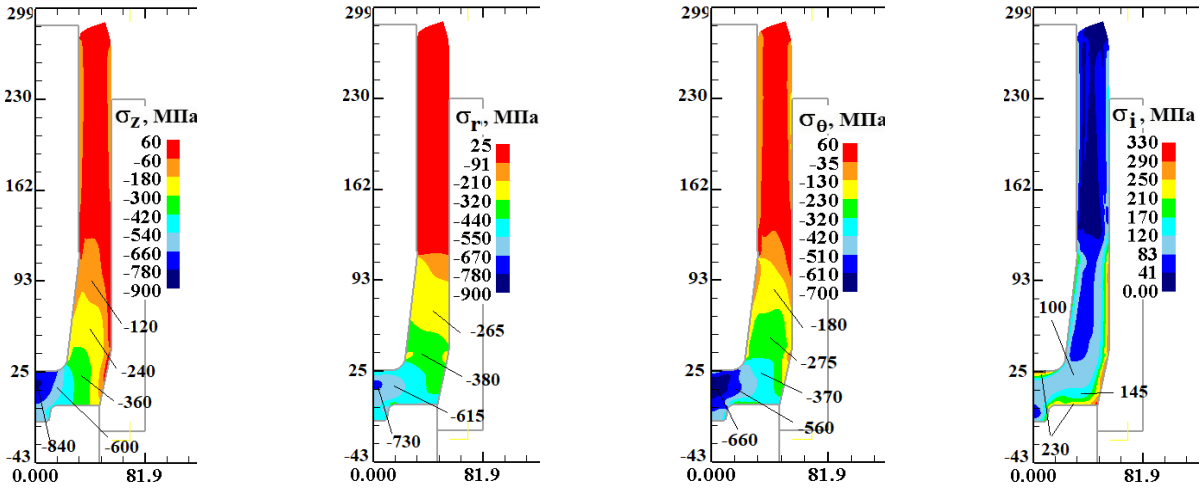

a b c d

Fig. 6. Distribution of stress components in a deformed workpiece at the end of reverse extrusion with upsetting under hot deformation conditions:
a – distribution of axial stresses σ_z, b – distribution of radial stresses σ_r,
c – distribution of tangential stresses σ_θ, d – distribution of stress intensity σ_i.

which is evident from the distribution pattern of stress intensity σ_i (Fig. 6d). In this part of the workpiece, the stress intensity is within the range σ_i = 140÷165 МПа.

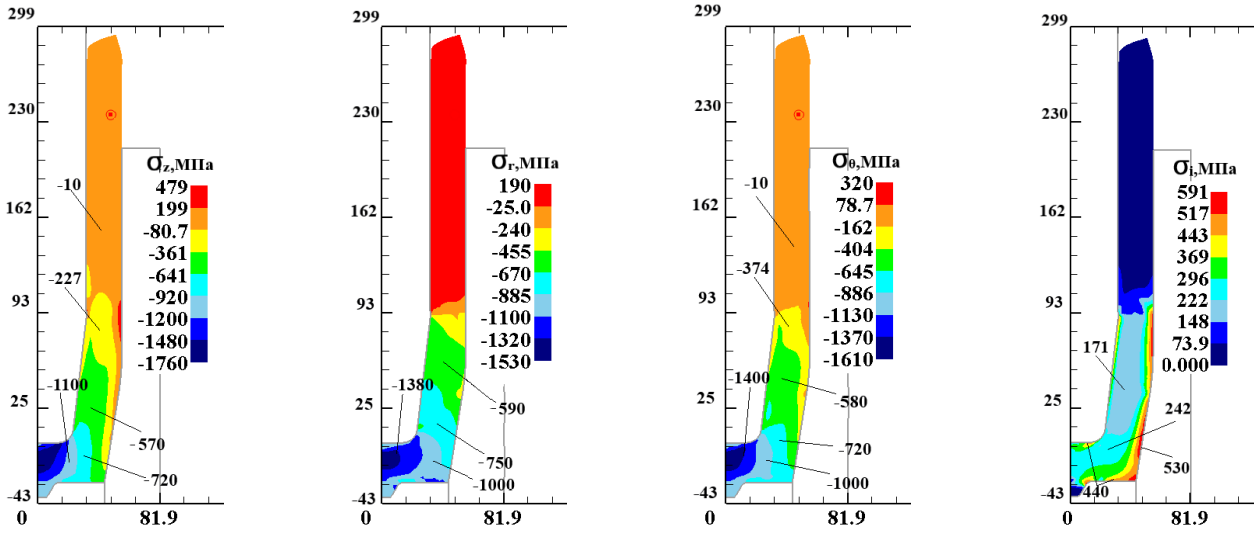

a b c d

Fig. 7. Distribution of stress components in a deformed workpiece at the end of reverse extrusion with upsetting under conditions of incomplete hot deformation:
a – distribution of axial stresses σ_z, b – distribution of radial stresses σ_r,
c – distribution of tangential stresses σ_θ, d – distribution of stress intensity σ_i.

The analysis of the distribution of stress components in the deformed blank at the end of incomplete hot reverse extrusion with upsetting relative to the axial stresses σ_z, radial stresses σ_r, tangential stresses σ_θ and stress intensity σ_i is shown in Fig. 7. As in hot deformation, in the deformation zone under the punch and between the conical part of the punch and the matrix, the axial stresses σ_z (Fig. 7a), radial stresses σ_r (Fig. 7b) and tangential stresses σ_θ (Fig. 7c) are compressive and significantly decrease in magnitude in the cylindrical part of the blank wall. As can be seen from the distribution of the stress state shown in Fig. 7a, in the bottom part of the blank under the punch, the axial deformation stresses are within σ_z = -570 ÷ -1700 МПа. The radial deformation stresses shown in Fig. 7b are within the range σ_r = - 750 ÷- 1380 МПа. The tangential deformation stresses shown in Fig. 7c are within the range σ_θ = -720 ÷ -1400 МПа. The deformations cover the entire bottom part of the workpiece, which is evident from the distribution of stress intensity σ_i (Fig. 7d). In this part of the workpiece, the stress intensity is within the range σ_i = 171 ÷ 440 МПа.

Fig. 8 and Fig. 9 show the distribution of deformations at the end of the process of hot and incomplete hot reverse extrusion with upsetting. The distributions of the final axial deformations ε_z, radial deformations ε_r, tangential deformations ε_θ and deformation intensity ε_i under hot reverse extrusion conditions are shown in Fig. 8. In the bottom part of the product, directly at the punch end, compressive axial deformations appear, which are within the range ε_z = -0.6 -2.4 (Fig. 8a). When a protrusion is formed on the bottom part of the product, tensile deformations are formed, reaching the value ε_z = 0.4. In the metal layers in the wall of the hole in the workpiece on the punch side, we obtain the value ε_z = –1, and along the wall thickness on the matrix side, tensile axial deformations ε_z arise. In Fig. 8b. The picture of the distribution of radial deformations is presented; in the cylindrical and conical parts of the wall of the product, compressive deformations equal to ε_r = - 0,88 arise.

In the metal layers on the punch side, the deformation values are equal to ε_r = -0,64 and change in thickness in the direction of the side surface on the matrix side to a value of ε_r = - 0,4. In the bottom part of the blank near the axis of symmetry, radial tensile deformations occur, which are within the limits of ε_r = 0,3÷0,8. Tangential deformations in the wall of the blank and the bottom part of the blank on the cavity side form tensile deformations (Fig. 8c). In the outer layers of the product wall metal on the matrix side, tangential deformations of ε_θ = 0,3 are obtained, increasing to ε_θ = 1,2 in the inner layers of the cavity metal.

In the bottom part of the workpiece, the deformations are in the range of ε_θ = 0,05 ÷ 1,6. On the boss of the bottom part of the workpiece, compressive deformations equal to ε_θ = -0,14 occur. The

degree of metal deformation under hot reverse extrusion conditions can be estimated using the distribution of deformation intensity ε_i shown in Fig. 8g. Intensive metal deformation is observed in the volume of the cylindrical and conical parts of the workpiece wall in layers close to the internal cavity of the workpiece ε_i = 1,2, with a subsequent decrease in the metal volume in the direction of the outer surface of the wall to ε_i = 0,43. Intensive deformation occurs in the bottom part of the workpiece cavity, where the deformation intensity value is in the range of ε_i = 0,43÷2,1. On the boss of the bottom the deformation intensity is in the range of ε_i = 0,11 ÷ 0,37.

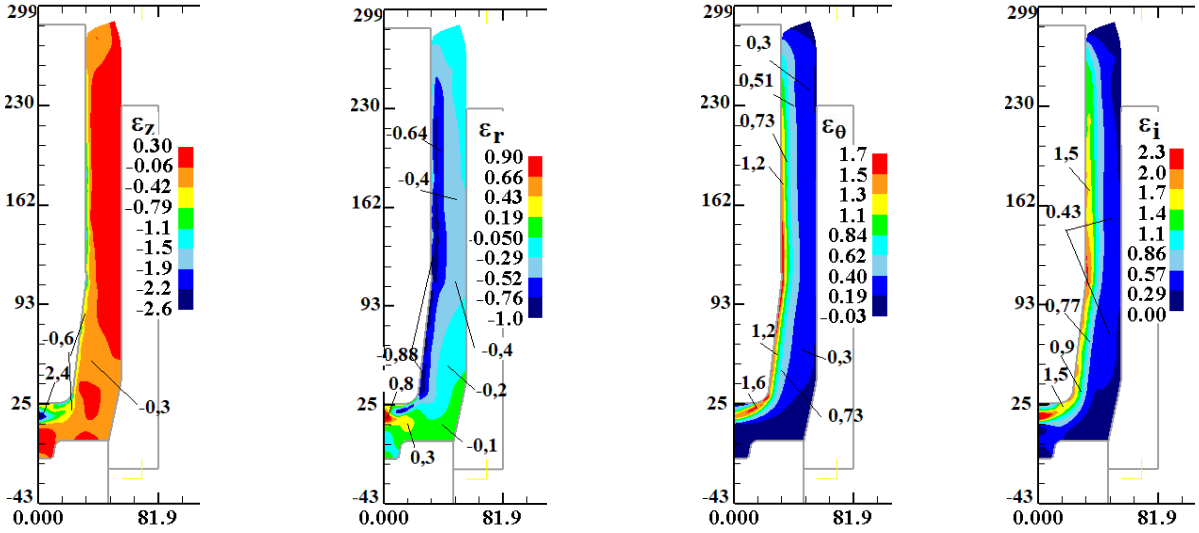

a b c d

Fig. 8. Distribution of final axial ε_z, radial ε_r, tangential ε_θ deformations and deformation intensity ε_i after hot reverse extrusion with upsetting:

a – distribution of axial deformations ε_z, b – distribution of radial deformations ε_r, c – distribution of tangential deformations ε_θ, d – distribution of deformation intensity ε_i.

Let us consider the distribution of the final axial strains ε_z, radial strains ε_r, tangential strains ε_θ and strain intensity ε_i under the conditions of incomplete hot reverse extrusion with upsetting shown in Fig. 9. Let us consider the deformed state that is formed in the bottom part of the semi-finished product, directly under the punch end, using axial strains that are within the range ε_z = - 0,1÷- 2,48 (Fig. 9a). When a protrusion is formed on the bottom part of the workpiece, the strains are of a stretching nature and reach values of ε_z = 0,4. In the thickness of the metal, the strains are equal to ε_z = -1. The next step is to consider the radial strains shown in Fig. 9b. In the cylindrical part of the workpiece and the conical parts of the wall of the workpiece, compressive deformations equal to the value of ε_r = -2,15 arise and increase in the direction of the outer surface ε_r = -0,4. In this part, tensile stresses of deformation arise, which are within the limits of ε_r = 0,8÷ -0,12. Tangential strains in the wall and bottom part of the part cause tensile stresses (Fig. 9c). In the thickness of the wall metal at the outer surface, tangential deformations equal to ε_θ = 0,08 are obtained, and in the internal layers of the metal, the accumulated tangential deformations are equal to ε_θ = 0,6 with a gradual decrease to ε_θ = -1,5 towards the cavity. In the volume of the bottom part of the workpiece, tangential deformations are within the limits of ε_θ = 0,09÷ 3,1. Due to the distribution of deformation intensity, it is possible to observe the worked structure of the metal during incomplete hot reverse extrusion.

The distribution of the deformation intensity is shown in Fig. 9d. In the cylindrical part of the product and the conical part, the metal deformation intensity from the inner side of the matrix cavity is εi = 0,2 with a subsequent increase in the value of εi = 0,72 towards the conical part. The deformation intensity in the bottom part under the punch is within εi = 2,68, and in the metal layers from the inner side of the workpiece, the deformation intensity is within εi = 1,2÷ 2,3. Deforming by extrusion with upsetting leads to intense deformations, which has a positive effect on the microstructure of the metal.

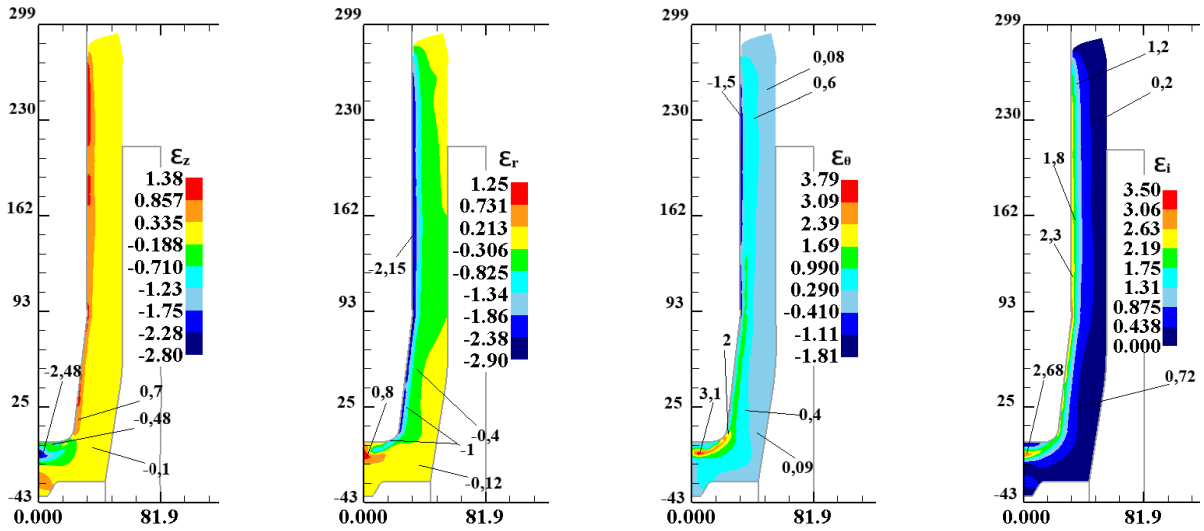

a b c d

Fig. 9. Distributions of final axial ε_z, radial ε_r, tangential ε_θ deformations and deformation intensity ε_i after incomplete hot reverse extrusion with upsetting:

a – distribution of axial deformations ε_z, b – distribution of radial deformations ε_r, c – distribution of tangential deformations ε_θ; d – distribution of deformation intensity ε_i.

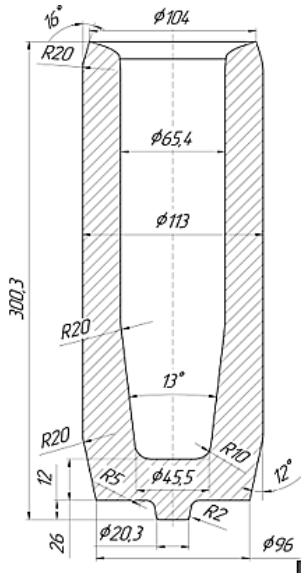

Fig. 10. Final shape and dimensions of the semi-finished product.

The final shape and dimensions of the product are shown in Fig. 10. According to the results of numerous experiments, the height of the finished hollow product differs by 1-1.5% with hot and incomplete hot extrusion. Since the dimensions and shape of the cavity are determined by the dimensions and geometry of the punch, the dimensions and geometry of the outer surface of the semi-finished product correspond to the geometry of the matrix, and the geometry and dimensions of the bottom correspond to the dimensions and geometry of the ejector. Sink marks are formed on the edge of the wall of the semi-finished product on the side of the cavity. To obtain a smooth end face of the wall of the semi-finished product, an additional trimming operation is required.

CONCLUSIONS

Using the finite element method and the plastic model of metal, mathematical models were created and a computer analysis of the processes of reverse extrusion with upsetting under hot and incomplete hot plastic deformation was performed. The extrusion forces were determined depending on the displacement of the punches. The maximum value of the extrusion forces under hot deformation was 2.4 MN, while under incomplete hot deformation the forces were 3.4 MN. The obtained results allow selecting pressing equipment and parameters of the die tooling. The distributions of specific forces on the contact surfaces of the deformed semi-finished product with the tool were established. The highest values of specific forces under hot and incomplete hot deformation reach the following values, respectively: on the matrices 490 and 718 MPa; on the punches 690 and 1490 MPa; on the ejectors 720 and 915 MPa. Based on the obtained results, recommendations were formulated on the number of matrix bandages and the selection of the required steel grade for the deforming tool in order to ensure the required strength. As a result of the study, distributions of components of stress and strain states and temperature in deformed metal of semi-finished products after hot and incomplete hot extrusion with upsetting were obtained.

During to the modeling of this deformation process, it was established that it is necessary to use tool heating. Also, the necessary parameters of the pressing equipment for ensuring the temperature regime were obtained, the need for accelerated movement of the pressing equipment was determined, which is ensured by upgrading the presses with hydraulic accumulators. The final shapes and sizes of semi-finished products after hot and incomplete hot extrusion with upsetting were determined, corresponding to the specified sizes of the semi-finished product.

REFERENCES

1. Qiyu Liao, Yanchao Jiang, Qichi Le, Lei Bao, Tong Wang, Lichen Liu, Yonghui Jia. Effect on the physical field of the die during the backward extrusion process of magnesium alloy wheel. *Materials Today Communications.* Volume 41. 2024. DOI: https://doi.org/10.1016/j.mtcomm.2024.110250
2. Danchenko V. N., Mylenyn A. A., Kuzmenko V. Y. Kompiuternoe modelyrovanye protsessov obrabotky metallov davlenyem. *Chyslennie metodi*. Dnepropetrovsk: Systemnie tekhnolohyy. 2008. 448 p.
3. Shewakh W. M. Effect of lubricant type on deep drawing ratio and drawing force during cylindrical cup drawing. *Emirates Journal for Engineering Research*. 2022. Vol. 27, № 3. P. 1-5.
URL: https://scholarworks.uaeu.ac.ae/ejer/vol27/iss3/3/
4. Kaliuzhnyi V.L., Alie va L.I., Yarmolenko O.S., Sytnyk S.V. Hot extrusion of high carbon steel cone hollow products. *Mech. Adv. Technol*. 6. 3. 2022, pp. 302–308. DOI: https://doi.org/10.20535/2521-1943.2022.6.3.269897
5. Voronko V. V., Shypul O. V. Proektyrovanye mnohoperekhodnoi shtampovky krыshky hydrotsylyndra s yspolzovanyem chyslennoho modelyrovanyia. *Zbirnyk naukovykh prats Kharkivskoho uni-versytetu Povitrianykh Syl.* Kh. : Kharkivskyi universytet Povitrianykh Syl imeni Ivana Kozheduba, 2008. Vyp. 3 (18). S. 14-19.
6. Noh Jeong-hoon, Hwang Beong-Bok Numerical analysis of tool geometry effect on the wear characteristics in a radial forward extrusion. *Journal of Mechanical Science and Technology*. 2015. 29. 8, pp 3447–3457. DOI: https://doi.org/10.1007/s12206-015-0743-4
7. Radkevych M.M., Fomin D., Hluchihin O. Doslidzhennia umov termomekhanichnoho protsesu nepovno hariachoho kuvannia. *Osnovni inzhenerni materialy* (tom 822), S. 165-170. DOI: https://doi.org/10.4028/www.scientific.net/KEM.822.165.
8. Hwang S.-F., Li Y.-R. Deep drawing behavior of metal-composite sandwich plates. *Materials*. 2022. Vol. 15. P. 6612. DOI: 10.3390/ma15196612
9. Emin Softić,. Emir Šarić Load force prediction of semi-hot combined extrusion process using finite element simulation. *7th International Research/Expert Conference "Trends in the Development of Machinery and Associated Technology" TMT 2013*. Istanbul, Turkey, 10-11 September 2013.
10. Malek Naderi, Mostafa Ketabchi, Mahmoud Abbasi, Wolfgang Bleak. Semi-hot Stamping as an Improved Process of Hot Stamping. Jour*nal of Materials Science & Technology*. Volume 27, Issue 4, April 2011, Pages 369-376.
11. Williams William M., Sandnes Lise, Ma Jun, Tronvoll Sigmund Arntsønn, Welo Torgeir. Yield stress and work hardening behavior of extruded AA6082 profiles under different homogenization and extrusion conditions. *Materials Research Proceedings*. 28 (2023) 467-476.
12. Aliieva L.I., Levchenko V.M., Aliiev I.S., Kartamyshev D.O. The development of triangular kinematic module to calculate the deformation pressure in the extrusion processes. *Materials working by pressure*. 2022. № 1(51) P. 10-20. DOI: 10.37142/2076-2151/2022-1(51)10
13. N.R. Chitkara, Aleem A. Extrusion of axi-symmetric tubes from hollow and solid circular billets: a generalised slab method of analysis and some experiments. *International Journal of Mechanical Sciences***.** Volume 43, Issue 7, (2001), Pages 1661-1684. DOI: https://doi.org/10.1016/S0020-7403(00)00093-X
14. Aleem A. Forward extrusion of monometallic and bi-metallic axi-symmetric tubular components using shaped dies and mandrels. *Ph.D. Thesis.* Universityof Manchester, April 1991.
15. Burden R. L., Faires J.D. Numerical Analysis. *3rd ed. P.W.S. Publications*, 1985.
16. Lee G. A., Im Y. T. Finite-element investigation of the wear and elastic deformation of dies in metal forming. *J. Mater. Process. Technol*., 89-90 (1999) 123-127.
17. B. A. Behrens, CIRP Ann. Finite element analysis of die wear in hot forging process. *Manuf. Technol*., 57 (1) (2008) 305-308.
18. Choi C. H., Groseclose A., Altan T. Estimation of plastic deformation and abrasive wear in warm forging dies. *J. Mater. Process. Technol*., 212 (8) (2012) 1742-1752.
19. Vardan O. C., Bagchi A., Altan T. Investigation of die wear in upsetting using FEM code ALPID. *Proc. 15th North American Manufac.* Res. Conf., SME Bethlehem, USA (1987) 386
20. Lange K., Cser L., Geiger M., Kals J. A. G., CIRP Ann. Tool life and tool quality in bulk metal forming. *Manuf. Tech.*, 41 (2) (1992) 667-675.
21. Drahobetskyi V.V., Kaliuzhnyi O.V., Kaliuzhnyi V.L., Sytnyk S.V. Vplyv shvydkosti deformuvannia na protses hariachoho vydavliuvannia z rozdachoiu kruhlykh porozhnystykh napivfabrykativ. Mechanics and Advanced Technologies. 2024. No. 1(100). P. 45–53. DOI: https://doi.org/10.20535/2521-1943.2024.8.1(100).297296
22. Miroslav P., Dragisa V., Milentije S.,Dejan M., Igor K. Orbital forging –aplausible alternative for bulk metal forming. *Journal of Trends in the Development of Machinery and Associated Technology*. Vol. 16, No. 1, 2012, ISSN 2303-4009.

Тітаренко А. Є., Горностай В. М., Святський Ю. Г., Ліподат В. Є. Вплив температури штампування при видавлюванні порожнистих виробів з високовуглецевої сталі.

В машинобудівному виробництві порожнистих виробів, використовують гаряче та неповне гаряче деформування. Основними технологіями виготовлення порожнистих виробів є видавлювання (екструзія), кування, штампування та спеціалізовані способи обробки металів тиском (ОМТ). До переваг процесів ОМТ, у порівнянні з процесами лиття, відносяться: мінімальні витрати матеріалів, висока якість матеріалу і поверхонь заготовки (процеси штампування і прокатка на прокатних станах), точність форми і розмірів, висока продуктивність, можливість механізації і автоматизації виробничих процесів. ОМТ на сучасному етапі розвитку технології машинобудування є одним з головних способів виготовлення деталей.

Зокрема, при виготовленні в сучасних умовах порожнистих виробів гостро постає потреба у визначенні параметрів штампового оснащення, його характеристик, технологічних переходів, температурних режимів обробки напівфабрикатів та їх взаємний плив на готовий виріб. Вказані питання розглядалися і продовжують розглядатися різними авторами, тому тема дослідження є актуальною. В запропонованій роботі виконано моделювання методом скінченних елементів процесу видавлювання порожнистих виробів із високовуглецевої сталі (AISI-1060) при гарячій та неповній гарячій деформації. Також виконано порівняння процесів зворотного видавлювання з осаджуванням в умовах гарячої та неповної гарячої деформації при відповідній постановці задачі для моделювання процесу зворотного видавлювання з осаджуванням при гарячій та неповній гарячій деформації. Аналіз результатів моделювання видавлювання дозволяє визначити характеристики отриманого виробу, зменшити час розробки технологічного процесу. Температура нагріву заготовки для моделювання видавлювання при гарячій деформації дорівнювала 1000 ºС, а для моделювання видавлювання при неповній гарячій деформації температура дорівнювала 700 ˚С. Зазначені температури визначені за допомогою діаграми стану, при температурі вище 760 ºС відбувається повна рекристалізація металу, це характерно гарячим процесам деформування, при температурі деформування нижче 760 ºС відбувається неповна рекристалізація, що характеризує процес неповного гарячого деформування. Результатами моделювання є залежності зусилля видавлювання від переміщення пуансона, величини нормальних напружень, за допомогою яких, встановлено питомі зусилля на контактуючих поверхнях між заготовкою та деформуючим інструментом, визначено розподіл температури в кінці процесу зворотного видавлювання порожнистого напівфабрикату та розглянуто розподіл напруженого та деформованого стану. Визначено потрібне пресове обладнання для отримання напівфабрикату та його кінцеву форму та розміри.

Ключові слова: *метод кінцевих елементів, гаряча деформація, неповна гаряча деформація, видавлювання при гарячій деформації, видавлювання при неповній гарячій деформації, порожнисті напівфабрикати, зусилля, питомі зусилля, напруження, деформації, температурний розподіл, схема видавлювання.*

Тітаренко Андрій Євгенійович – аспірант КПІ ім. Ігоря Сікорського
Titarenko Andrii – aspirant of Igor Sikorsky Kyiv Polytechnic Institute
E-mail: k_OMD@ukr.net
ORCID: https://orcid.org/0000-0002-0407-5144

Горностай Вадим Миколайович – канд. техн. наук, доцент кафедри технології виробництва літальних апаратів НТУУ КПІ ім. Ігоря Сікорського
Hornostay Vadym – Candidate of Technical Sciences, Associate Professor, Igor Sikorsky Kyiv Polytechnic Institute
E-mail: w.gornostay@kpi.ua
ORCID: https://orcid.org/0000-0001-5766-931X

Святський Юрій Георгійович – аспірант НТУУ КПІ ім. Ігоря Сікорського
Sviatskyi Yurii – aspirant of Igor Sikorsky Kyiv Polytechnic Institute
E-mail: k_OMD@ukr.net
ORCID: https://orcid.org/0009-0008-7167-5925

Ліподат Віталій Євгенович – аспірант НТУУ КПІ ім. Ігоря Сікорського
Lipodat Vitaliy – aspirant of Igor Sikorsky Kyiv Polytechnic Institute
E-mail: k_OMD@ukr.net
ORCID: https://orcid.org/0009-0004-3986-4794

НТУУ «КПІ ім. Ігоря Сікорського» – Національний технічний університет України «Київський політехнічний інститут імені Ігоря Сікорського», м. Київ
NTUU "Igor Sikorsky KPI" – National Technical University of Ukraine "Igor Sikorsky Kyiv Polytechnic Institute", Kyiv

Стаття надійшла до редакції 12.07.25.